Available online at www.sciencedirect.com
SCIENCE DIRECT®
Bioelectrochemistry 59 (2003) 73–84
Bioelectrochemistry
www.elsevier.com/locate/bioelechem

A new computational approach for electrical analysis of biological tissues

Airton Ramos[a,b,*], Adroaldo Raizer[c], Jefferson L.B. Marques[b]

[a] Centre of Technological Sciences, Electrical Engineering Department, State University of Santa Catarina (UDESC), Santa Catarina, Brazil
[b] Institute of Biomedical Engineering, Department of Electrical Engineering, Federal University of Santa Catarina (UFSC), Santa Catarina, Brazil
[c] Laboratory of Electromagnetic Compatibility, Department of Electrical Engineering, Federal University of Santa Catarina (UFSC), Santa Catarina, Brazil

Accepted 16 January 2003

Abstract

A new computational approach for electrical analysis especially designed for application in biological tissues is presented. It is based on the modelling of the electrical properties of the medium by means of lumped circuit elements, such as capacitance, conductance and current sources. The cell scale model is suitable for modelling the local anisotropy around cell membranes. It permits to obtain the electric potential, ionic concentrations and current densities around cells in time steps in an iterative process. The tissue scale model utilises volume-averaged values of conductivity and permittivity and models suitably the dispersive characteristic of biological tissues. It permits to obtain potential and current distributions in large volumes of tissue in the time or frequency domain. An example of analysis of skeletal muscle is presented aiming to demonstrate the features of the method.

Keywords: Bioelectromagnetism; Biological system modelling; Field calculation

1. Introduction

Numerical field calculation is an important tool in the electromagnetic characterisation of living matter. About this subject, most of works produced up to now have focused on the estimate of the power absorption by organs or the entire body inside an electromagnetic field [1]. Because the analysed volume is very large compared with the cell dimensions, the tissues involved are usually taken as homogeneous relatively to their electromagnetic properties. Nevertheless, when the focus is on the effect of the applied field on individual cells, it demands high spatial resolution analysis with suitable modelling of the electric properties of the medium, in order to account correctly the local anisotropy around cells.

Electrical properties of biological tissues are complex. In the scale of cell dimensions, the lipidic membranes act as barriers for the movement of ions. Charge accumulation on interfaces electrolyte–membranes causes field distortions, conductivity increases and diffusive fluxes of ions around the cells. Furthermore, the extension of the problem is increased by the morphological complexity of the cells. Cell shapes are irregular. Biological membranes are very thin structures (about 10 nm) compared with the total cell dimensions (cell radius ranges from about 5 to 150 μm). Double layers, the regions of charge accumulation around interfaces, are even thinner (about 1 nm). Besides, biological tissues generally present strong dispersive behaviour of their electrical properties from very low to microwave frequencies.

In this paper, the equivalent circuit method (ECM) for computational electrical analysis is presented. It was designed aiming to obtain suitable numerical modelling of the electric transport process, local anisotropy around cell membranes and biological interfaces and dispersive behaviour of tissues. It is divided into two approaches: (1) cell scale model is based on the modelling of the electric transport properties of the medium by means of lumped circuit elements as capacitance, conductance and current sources, representing the displacement, drift and diffusion currents, respectively; (2) tissue scale model is based on the modelling of the dispersive behaviour of tissues by means of a network of lumped capacitances and conductances.

An important feature of the method is the facility to model boundary conditions and interfaces by simply connecting circuit elements from each one of the adjacent mediums. Besides, it is very easy to understand and implement in a computer program.

* Corresponding author. Centre of Technological Sciences, Electrical Engineering Department, State University of Santa Catarina (UDESC), Santa Catarina, Brazil.
E-mail addresses: dee2ar@joinville.udesc.br (A. Ramos), raizer@eel.ufsc.br (A. Raizer), jmarques@ieb.ufsc.br (J.L.B. Marques).

1567-5394/03/$ - see front matter © 2003 Elsevier Science B.V. All rights reserved.
doi:10.1016/S1567-5394(03)00004-5

2. Equivalent circuit method—cell scale model

In order to obtain the equivalent electric circuit of a medium in the cell scale model, initially, the volume under analysis should be divided in a large number of small blocks with parallelepiped shape, as shown in Fig. 1. Each block constitutes a node in an equivalent circuit and communicates with its neighbours by means of a set of paralleled circuit elements: a conductance and a current source for each kind of electric charge carrier in the medium, modelling the conduction and diffusion currents, respectively, and a capacitance representing the displacement current. Each element is calculated based on the dimensions of the block and the electric and transport properties in that point of the space. In this discretized space, the total current leaving each node of the circuit is given by the following difference equation:

$$I = \sum_i \sum_n (g_{ni}\Delta_i V + k_{ni}\Delta_i \rho_n) + \sum_i C_i \frac{\delta(\Delta_i V)}{\delta t} \tag{1}$$

where the index n identifies each type of charge carrier in the medium and i identifies each direction of the space ($i = x,y,z$). V is the electric potential and ρ is the charge density inside a block. Δ and δ indicate difference in space and time, respectively. The parameters g, k and C are the conductance, diffusion coefficient and capacitance of the block, respectively, and they are given by:

$$g_{ni} = \rho_n \mu_{ni} \frac{A_i}{L_i}, \quad k_{ni} = f_n D_{ni} \frac{A_i}{L_i}, \quad C_i = \varepsilon_i \frac{A_i}{L_i} \tag{2}$$

where μ_n and D_n are the mobility and diffusion coefficients of the charge carrier n and ε is the permittivity of the medium. A and L are the area and length at the connection of two adjacent blocks and f_n is a voltage-dependent factor from the solution of the one-dimensional Nerst–Planck equation between two nodes (see Appendix A).

The electric potential, currents and charge distributions can be obtained by solving the resulting electric circuit in time steps in an iterative process. Defining I_{qn} as the part of the total current due to the movement (diffusion + conduction) of the n type charge carriers and applying the Kirchhoff Current Law to the central node (node O) in Fig. 1, we obtain:

$$\begin{aligned} &C_{\mathrm{ON}} \frac{\delta(V_{\mathrm{O}} - V_{\mathrm{N}})}{\delta t} + \sum_n I_{qn\mathrm{ON}} + C_{\mathrm{OS}} \frac{\delta(V_{\mathrm{O}} - V_{\mathrm{S}})}{\delta t} \\ &\quad + \sum_n I_{qn\mathrm{OS}} + C_{\mathrm{OW}} \frac{\delta(V_{\mathrm{O}} - V_{\mathrm{W}})}{\delta t} + \sum_n I_{qn\mathrm{OW}} \\ &\quad + C_{\mathrm{OE}} \frac{\delta(V_{\mathrm{O}} - V_{\mathrm{E}})}{\delta t} + \sum_n I_{qn\mathrm{OE}} + C_{\mathrm{OU}} \frac{\delta(V_{\mathrm{O}} - V_{\mathrm{U}})}{\delta t} \\ &\quad + \sum_n I_{qn\mathrm{OU}} + C_{\mathrm{OD}} \frac{\delta(V_{\mathrm{O}} - V_{\mathrm{D}})}{\delta t} + \sum_n I_{qn\mathrm{OD}} = 0 \end{aligned} \tag{3}$$

This equation can be rewritten in a more simplified and suitable way for computation:

$$\begin{aligned} &(C_{\mathrm{ON}} + C_{\mathrm{OS}} + C_{\mathrm{OW}} + C_{\mathrm{OE}} + C_{\mathrm{OU}} + C_{\mathrm{OD}})V_{\mathrm{O}} \\ &\quad - C_{\mathrm{ON}}V_{\mathrm{N}} - C_{\mathrm{OS}}V_{\mathrm{S}} - C_{\mathrm{OW}}V_{\mathrm{W}} - C_{\mathrm{OE}}V_{\mathrm{E}} - C_{\mathrm{OU}}V_{\mathrm{U}} \\ &\quad - C_{\mathrm{OD}}V_{\mathrm{D}} = Q_{\mathrm{O}} \end{aligned} \tag{4}$$

where Q_{o} is the total charge in the volume of the central block, which is calculated in each time step by:

$$Q_{\mathrm{o}}^{\mathrm{actual}} = Q_{\mathrm{o}}^{\mathrm{former}} - \sum_M \sum_n I_{qn\mathrm{OM}} \delta t \tag{5}$$

where M indicates each neighbour node connected to the central node through the branch OM. Currents are considered positive when leaving the central node. Likewise, the charge density for each charge carrier type in the medium can be obtained by means of finite integration, according to the equation:

$$\rho_n^{\mathrm{actual}} = \rho_n^{\mathrm{former}} - \left(\frac{1}{\Delta v}\right) \sum_M I_{qn\mathrm{OM}}\ \delta t \tag{6}$$

where Δv is the volume of that block.

Based on the model represented by Eqs. (1) and (2), an equivalent circuit between adjacent nodes is proposed in Fig. 2. Then, the ECM in the cell scale model consists in obtaining the equivalent circuit of the medium and to solve the system of equations as Eq. (4), one for each node of the equivalent circuit, in time steps, for the given boundary and initial conditions, and to update the total charge and charge densities in each step, according to Eqs. (5) and (6). The conductance g_n for each charge carrier should be updated too, utilising the new values of charge densities.

The whole set of node equations (Eq. (4)) can be written in a compact form, using matrix notations:

$$CV = Q + F \tag{7}$$

where C is a capacitance matrix $N \times N$ (N is the number of nodes of the circuit) containing the coefficients of node potentials according to Eq. (4) (see Appendix C). V and Q

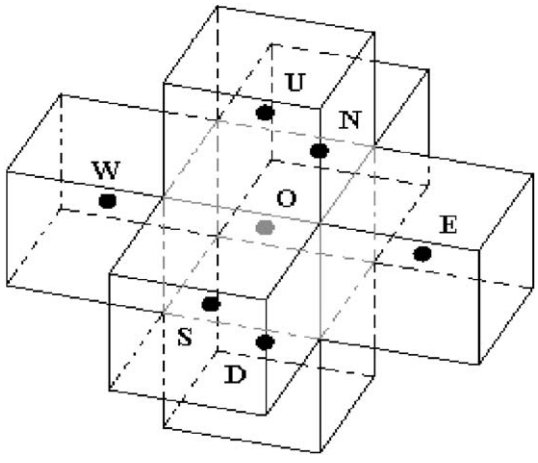

Fig. 1. Space discretization in a parallelepiped block mesh.

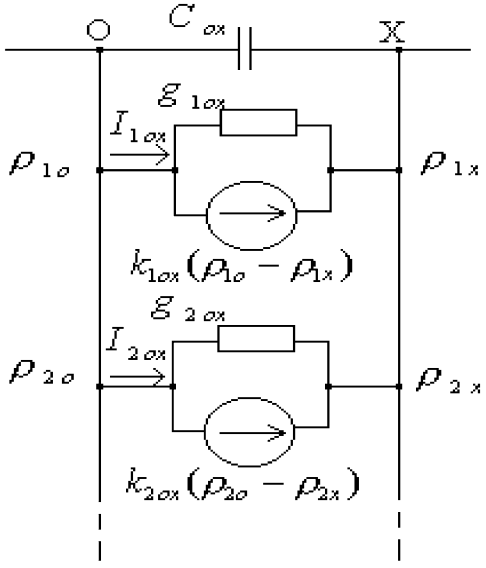

Fig. 2. Equivalent circuit for cell scale model. The letters O and X indicate nodes of the circuit. The numbers 1 and 2 indicate different charge carrier types.

are vectors of node potential and total charge. F is the excitation vector, defined by:

$$F = \begin{bmatrix} C_{F1}V_{F1} \\ C_{F2}V_{F2} \\ \cdots \\ C_{FN}V_{FN} \end{bmatrix} \tag{8}$$

where C_{FN} is the capacitance connecting the source electrode to the medium and V_{FN} is the source potential in node n. According to Eq. (7), the potential vector is obtained from:

$$V = C^{-1}(Q + F) \tag{9}$$

Naturally, since geometry and permittivity of the medium do not change during processing, C is constant and its inverse form can be obtained once at the beginning of the calculation. On the other hand, Q and F should be updated in each iteration.

3. Time step and convergence

Convergence of the iterative process is possible only if the time step is smaller than some convergence threshold, determined by the charging kinetic on the interfaces of the medium. This can be evaluated from the continuity equation:

$$\frac{\partial \rho}{\partial t} = -\nabla(J_c + J_d) = -\nabla(\sigma E + D\nabla\rho) \tag{10}$$

where ρ is the total charge density, J_c and J_d are the conduction and diffusion current density, respectively. σ is the conductivity and D is the average diffusion coefficient (calculated over all kind of charge carriers) in that point of the space. We can obtain an estimate of the contribution of these two processes, conduction and diffusion, to the charging rate, making an approximate analysis valid in the initial instants of the interface charging. For a flat interface perpendicular to the applied field, as shown in Fig. 3, the interface is rapidly charged in the initial instants after turning on the source, while the neighbourhood remains essentially neutral. So, the diffusion current density leaving the interface can be given approximately by:

$$J_d = (2D/\Delta x)\rho_s \tag{11}$$

where ρ_s is the accumulated charge density in the region adjacent to the interface and Δx is the discretization length of the space. Then, according to Eq. (10), the contribution of this process to the charging rate is:

$$\frac{\partial \rho_s}{\partial t} = -\nabla J_d = -(2D/\Delta x^2)\rho_s \tag{12}$$

and we can define a diffusion relaxation time at the interface by:

$$\tau_{sd} = \Delta x^2/2D \tag{13}$$

Furthermore, there is conduction current leaving the interface due the electric field produced by the accumulated charge:

$$J_c = (\sigma \Delta x/2\varepsilon)\rho_s \tag{14}$$

and likewise the diffusion current, this conduction current contributes to the interface charging kinetics with the conduction relaxation time:

$$\tau_{sc} = 2\varepsilon/\sigma \tag{15}$$

Then, the total relaxation time for the charging process at the interface is:

$$\tau_s = \tau_{sd}\tau_{sc}/(\tau_{sd} + \tau_{sc}) = (2\varepsilon/\sigma)/(1 + 4(L_D/\Delta x)^2) \tag{16}$$

where $L_D = \sqrt{\varepsilon D/\sigma}$ is the Debye length, which for a physiological electrolyte is about 1 nm (10^{-7} cm). Eq. (16)

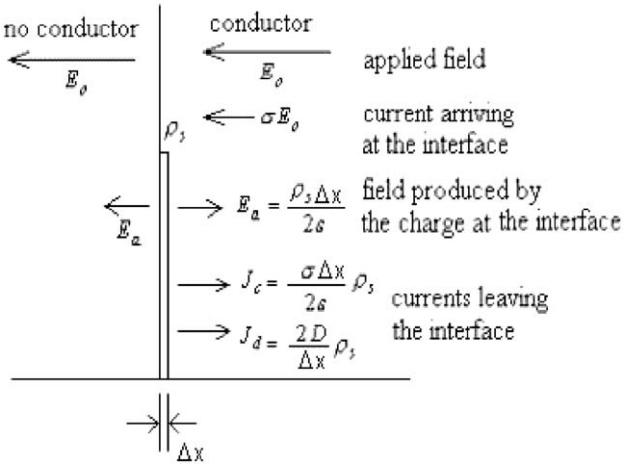

Fig. 3. Schematic representation of the charging process of a plan interface at the initial instants.

shows that the numerical evaluated charging kinetics is dominated by the conduction process for $\Delta x \gg L_D$. However, in high-resolution analysis, where Δx is of the order or lower than L_D, the diffusion process plays an important role in the numerical results. For other surfaces different from a flat, τ_s can be smaller than that value from Eq. (16). Then, the rule for convergence is $\Delta t < \tau_s$.

4. Two-dimensional modelling of a skeletal muscle

The method described above permits local analysis around cell membranes and subcellular structures. As an example of its applicability, we analysed a simplified model of a skeletal muscle tissue. Fig. 4 shows a schematic representation of the skeletal muscle in a transversal plane. For the purpose of this study, the tissue is only a group of very thin isolating membranes immersed in aqueous solution of ions. The geometrical details of a group of muscle fibres inside a bundle are also shown. Because of the symmetries, local analysis can be made just in the rectangular region shown in that figure. Cell radius is assumed to be 50 μm and minimum distance between neighbour cells is 1 μm. The cell marked with the angle α is the target for local and averaged calculation of electric field and currents. Only the influence of the nearest neighbour cells are considered in the calculation on the target cell. Electric properties of the medium are given in Table 1.

The discretization mesh for this two-dimensional problem was built with two levels of resolution, using square elements. As shown in Fig. 5, the low-resolution mesh occupied the major area far from the membranes. In order to obtain a good representation of the geometrical details in the interstitial space, a high-resolution mesh was built around the membranes.

Table 1
Electrical properties of the medium

Parameter	Value
Ionic density (intra- and extracellular)	Na^+ 0.14 M (13.5 C cm^{-3}), Cl^- 0.14 M (13.5 C cm^{-3})
Ionic mobility in water[a]	Na^+ 5.2×0^{-4} cm^2 V^{-1} s^{-1}, Cl^- 7.9×10^{-4} cm^2 V^{-1} s^{-1}
Ionic diffusion coefficient in water[a]	Na^+ 1.33×10^{-5} cm^2 s^{-1}, Cl^- 2.03×10^{-5} cm^2 s^{-1}
Eletrolyte permittivity[b]	78
Membrane capacitance[c]	10^{-6} F cm^{-2}

Physiological composition is simplified for only two ions. Values in parentheses are the equivalent charge densities.
[a] Values for 298 K from [3].
[b] It was considered only the water contribution.
[c] Typical value for biological membranes from [2].

In the whole analysed region, there are 92 × 50 divisions in the x and y direction, respectively, resulting in 4600 square elements of edge $h = 1.75$ μm. In the high-resolution region, there are 25 small squares inside each big one. The total number of elements in the mesh is 12,664. Each element defines a node of the equivalent circuit of the medium. The number of connections for each node depends on its position in the mesh. It is 3 for nodes on the even symmetry planes. For big elements in the bulk, this number is 4 for those not in contact with the high-resolution region or 8, 12 or 16, otherwise. So, the number of terms in each node equation of the circuit ranges from 4 to 17. When two neighbour elements are in opposite sides of the membrane, the connection between them are made only by the membrane capacitance.

Boundary conditions are specified in the inset of Fig. 4. Planes A and B are for source connection. Field and currents vanish on planes C and D because geometrical symmetry

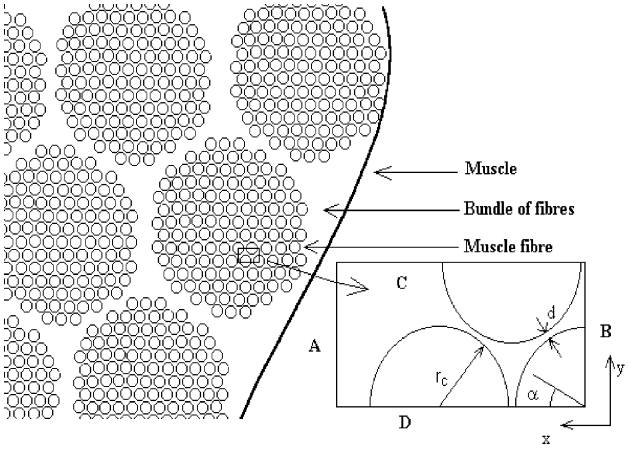

Fig. 4. Schematic representation of a skeletal muscle in a transversal plane. Local analysis was performed in the rectangular region inside the bundle. The source of potential was connected to plane A. The source reference (0 V) was connected to plane B. In the planes C and D, currents and field vanish due to the even symmetry of charge and potential distribution. For dog skeletal muscle, $r_c \approx 50$ μm [2] and d was fixed arbitrarily at 1 μm.

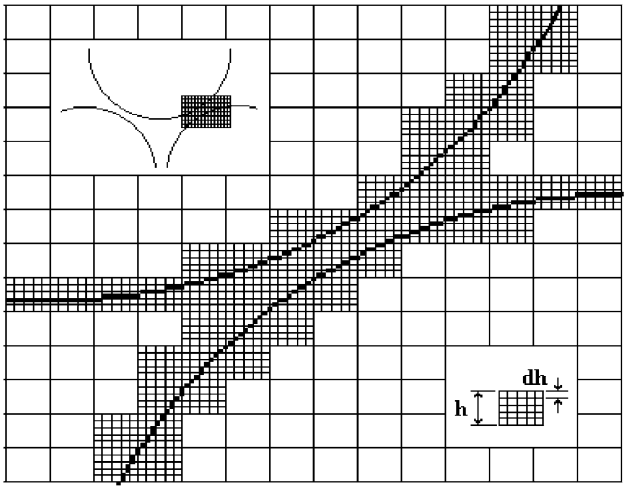

Fig. 5. Expanded view of a small region of the discretization mesh. In the present case, $h = 5dh$, so that there are 25 small squares inside a big one.

results in even symmetry for potential and charge distribution around them.

5. Results using the cell scale model

In the first numerical experiment, an electric field as a step of 100 V/cm was applied in the x direction. The potential in the plane A was calculated considering $V=0$ in the plane B. It was executed 2000 iterations with time step of 0.3 ns. The distribution of potential in steady state is shown in Fig. 6. As it was expected, the potential is constant inside cells while membranes support the major part of the potential drop. Because the membrane is very thin, the electric field on it is much higher than the applied field on the tissue. Electric field on the membranes in steady state is shown in Fig. 7, as a function of the angle α. In Fig. 8, the electric field in $\alpha=0$ is shown as a function of the time. In both graphs, the corresponding results for a single cell obtained from numerical and theoretical calculations are also shown. The theoretical analysis is shown in Appendix B.

Agreement between numerical and theoretical field distribution in steady state for a single cell is good. Error is about 3% in $\alpha=0$. Nevertheless, in the tissue, field distribution is very different from the theoretical cosine distribution. This electric field results from charge accumulation on membrane surfaces, but transversal flux of ions is reduced in some regions where membranes are very close.

Time constant for membrane charging obtained from numerical simulation for the single cell departs from theoretical value by about 15%. This is significantly higher than the field amplitude error, what suggests a stronger dependence of the numerically evaluated charging kinetics from mesh resolution. On the other hand, charging kinetics in the tissue is more complex, because it runs approximately as a second order relaxation process. According to the numerical simulation results, electric field on the membrane can be written in the form:

$$E_m = E_1(1-\exp(-t/\tau_1)) + E_2(1-\exp(-t/\tau_2)) \qquad (17)$$

Values for (E_1, τ_1) and (E_2, τ_2) are shown in Fig. 8 and they were used for tracing the continuous line curve for the

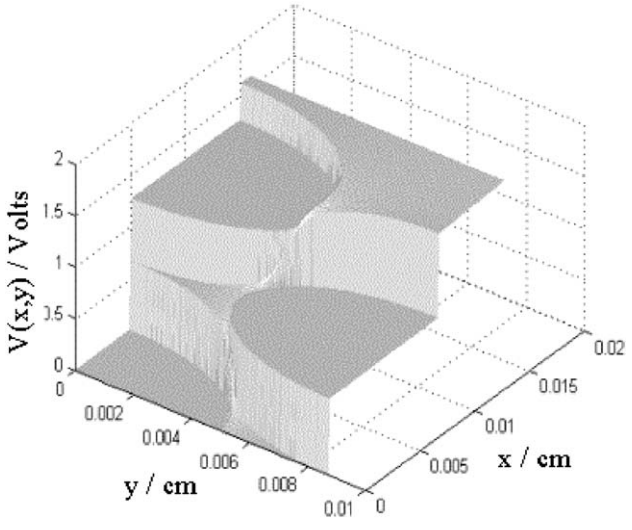

Fig. 6. Potential distribution 6 μs after an electric field step of 100 V/cm in the x direction.

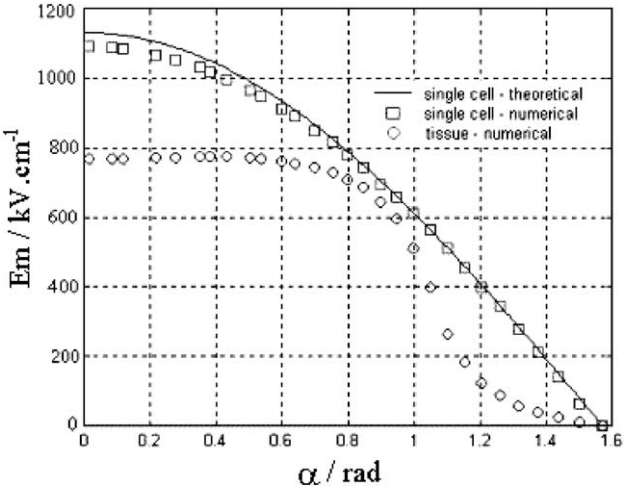

Fig. 7. Electric field distribution on the membrane of the target cell in the tissue and in a single cell obtained both in the same electrolyte composition and applied field of 100 V/cm. α is the angle between electric field and position vector on the membrane. The theoretical curve for a single cell is based on the analysis shown in Appendix B. In order to get the membrane capacitance of 1 μF/cm^2, we used the value 8.85 nm for the membrane thickness and 10 to the membrane permittivity.

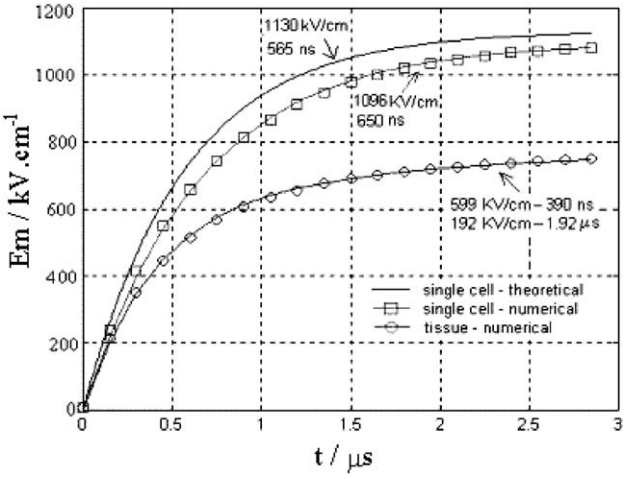

Fig. 8. Time dependence of the electric field on the membrane in $\alpha=0$ for the target cell in the tissue and in a single cell obtained both in the same electrolyte composition and applied field of 100 V/cm. The theoretical curve for a single cell is based on the analysis shown in Appendix B. Continuous line in numerical results represents the best fit for an analytical second order model (Eq. (17)).

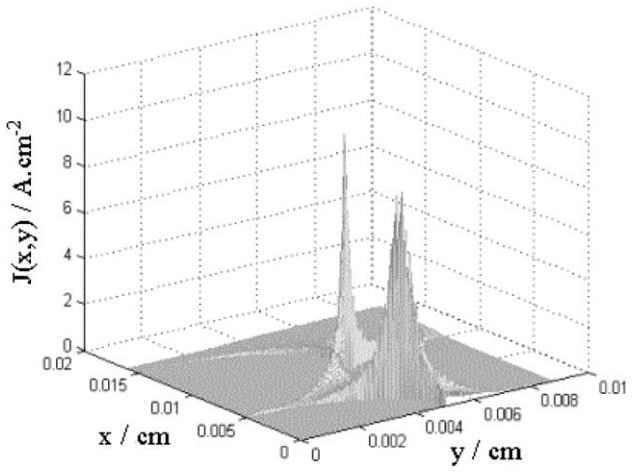

Fig. 9. Current distribution 6 μs after an electric field step of 100 V/cm in the x direction.

tissue. These parameters were observed to be dependent of angle α.

Fig. 9 shows the total current density (absolute value) distribution in steady state. Because membranes are very thin, immediately after the step, the current distributes almost uniformly in the space. However, as membranes are charged, the current is concentrating in the interstitial space between cells. A plot of the time evolution of the averaged value of the current density in the x direction is shown in Fig. 10. This average was calculated in the marked region (inset on Fig. 10). As will be demonstrated, this behaviour can be modelled very well as a first order relaxation process.

In the second numerical experiment, the applied electric field was a pulse of 100 V/cm and duration 30 ns. Fig. 10 shows the averaged total current in the x direction as a function of time. Using Fourier transform, we can obtain the

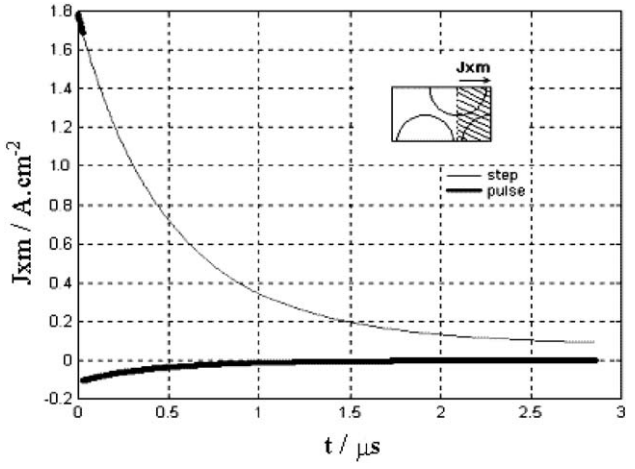

Fig. 10. Time dependence of the averaged current density in the x direction for step and pulse excitation. Averaged values were calculated on the marked region shown in the inset.

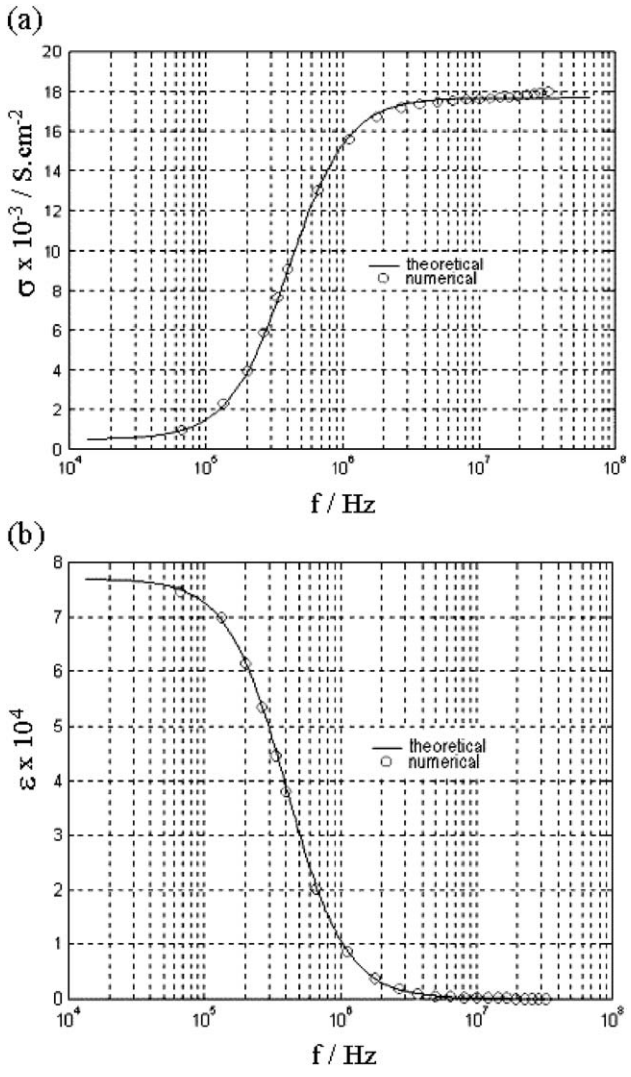

Fig. 11. Frequency dependence of (a) averaged conductivity and (b) averaged permittivity in a bundle of skeletal muscle fibres according to the numerically obtained field and current distribution around the target cell. The theoretical curves are the best fit for the first order relaxation model given by Eqs. (21) and (22) with $\sigma_s = 4.7 \times 10^{-4}$ S/cm, $\Delta\sigma = 1.72 \times 10^{-2}$ S/cm, $\varepsilon_\infty = 78$, $\Delta\varepsilon = 7.7 \times 10^4$ and $\tau = 0.4$ μs.

frequency dependence of the averaged tissue conductivity and permittivity inside a bundle of fibres. The tissue specific admittance is given by:

$$\gamma(\omega) = J(\omega)/E(\omega) = \sigma(\omega) + j\omega\varepsilon_o\varepsilon(\omega) \tag{18}$$

where ω is the angular frequency, J is the averaged current density, E is the averaged electric field, $j = \sqrt{-1}$ and $\varepsilon_o = 8.85 \times 10^{-14}$ F/cm. Then, σ and ε are given by:

$$\sigma(\omega) = Re[\gamma(\omega)] \tag{19}$$

$$\varepsilon(\omega) = Im[\gamma(\omega)]/\omega\varepsilon_o \tag{20}$$

Fig. 11 shows the obtained $\sigma(\omega)$ and $\varepsilon(\omega)$. The continuous line in those graphs represents the best fit for the first order relaxation model given by [2,4]:

$$\sigma(\omega) = \sigma_s + \Delta\sigma\omega^2\tau^2/(1+\omega^2\tau^2) \quad (21)$$

$$\varepsilon(\omega) = \varepsilon_\infty + \Delta\varepsilon/(1+\omega^2\tau^2) \quad (22)$$

where σ_s is the static conductivity and ε_∞ is the relative permittivity in high frequencies. $\Delta\sigma$ and $\Delta\varepsilon$ are the conductivity and permittivity amplitudes of dispersion respectively and τ is the time constant of the relaxation process. $\Delta\sigma$ and $\Delta\varepsilon$ are interrelated by:

$$\Delta\varepsilon = (\tau/\varepsilon_o)\Delta\sigma \quad (23)$$

Using $\varepsilon_\infty = 78$, the values obtained for the other parameters are: $\sigma_s = 4.7\times10^{-4}$ S/cm, $\Delta\sigma = 1.72\times10^{-2}$ S/cm, $\Delta\varepsilon = 7.7\times10^{4}$ and $\tau = 0.4$ μs. These are in qualitative agreement with experimental results and theoretical calculations for the β dispersion of the dog skeletal muscle [2].

6. Equivalent circuit method—tissue scale model

The method presented above applies to the analysis in the scale of cell dimensions. Because it demands high-resolution meshes, it is unsuitable for analysis of large volumes of tissue. When dealing with tissues, since the focus is no longer cells, but large amount of cells, an averaged volume electrical properties based model is more suitable. Fig. 11 shows that the averaged conductivity and permittivity of an cylindrical cell aggregate is very well described by a first order relaxation model. However, dielectric properties of real biological tissues are more complex. Besides the β dispersion shown above, real tissue normally presents the α dispersion in very low frequencies associated with ionic diffusion in double layers around plasmatic membranes and γ dispersion related mainly to the water polar relaxation, which occurs in microwave frequencies [2,4]. Because those processes occur in very different frequency ranges, generally, they can be well approached by independent first order relaxation models [4]. However, many tissues are better modeled by fitting some empirical relaxation function as that proposed by Cole and Cole [5], which nevertheless lacks theoretical justification.

In the simplest case, when dealing with independent relaxation processes with relaxation times well separated, the dielectric response of the tissue can be modelled by the equations [2]:

$$\sigma(\omega) = \sigma_s + \Delta\sigma_\alpha\frac{\omega^2\tau_\alpha^2}{1+\omega^2\tau_\alpha^2} + \Delta\sigma_\beta\frac{\omega^2\tau_\beta^2}{1+\omega^2\tau_\beta^2} + \cdots \quad (24)$$

$$\varepsilon(\omega) = \varepsilon_\infty + \frac{\Delta\varepsilon_\alpha}{1+\omega^2\tau_\alpha^2} + \frac{\Delta\varepsilon_\beta}{1+\omega^2\tau_\beta^2} + \cdots \quad (25)$$

where $\Delta\sigma$ and $\Delta\varepsilon$ for each band are interrelated by Eq. (23).

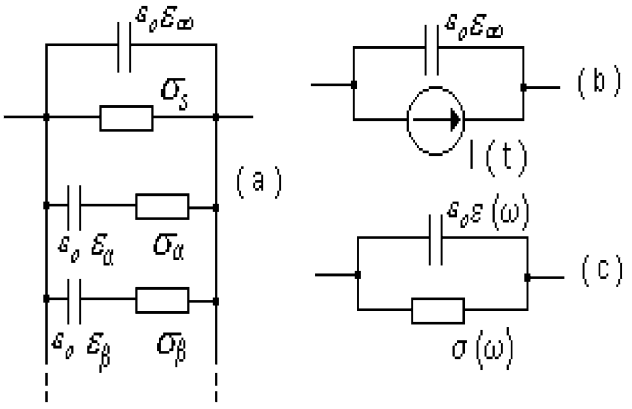

Fig. 12. (a) Equivalent circuit to model the dispersive properties of a medium in the tissue scale model with any bands of independent first order relaxation. In order to obtain the correct values for the circuit elements, each parameter in the model should be multiplied by the geometrical factor A/L, where A is the transversal area and L is the length for each specific connection. (b) Simplified circuit for time domain analysis. (c) Simplified circuit for frequency domain analysis.

The tissue scale model for numerical analysis of biological media is based on the above described model. An equivalent circuit where any number of independent relaxation bands can be modelled is proposed in Fig. 12. The method consists in the space discretization and connection of each element with its neighbours through the equivalent circuit in Fig. 12(a), multiplying each parameter in the model by the geometrical factor A/L, where A is the transversal area and L is the length for each specific connection. The resultant circuit can be analysed by any method from linear circuit theory. The two approaches that we have used are presented.

6.1. Iterative method for time domain analysis

This approach is equivalent to the method presented in the first part of this paper. Circuit of Fig. 12(a) is simplified to that of Fig. 12(b) where the capacitance in high frequency is preserved, but all other elements are considered to be related to the time dependent conduction current between nodes of the circuit. Taking only two relaxation bands in the model, this current can be evaluated as follows:

$$I(t) = g_s V_{ox} + I_\alpha + I_\beta \quad (26)$$

where $g_s = \sigma_s A/L$, V_{ox} is the potential difference between nodes (these nodes were named 'o' and 'x'). I_α and I_β are the dispersive currents. They can be evaluated by an iterative method. Given a small incremental step in the current of any dispersive branch in Fig. 12(a), the increment in the potential difference between nodes in the time interval Δt is given by:

$$\delta V_{ox} = (I(t)/c)\delta t + \delta I/g \quad (27)$$

where $c = \varepsilon_o\varepsilon A/L$ and $g = \sigma A/L$. Then, the current in $t+\delta t$ can be written as:

$$I(t+\delta t) = I(t) + \delta I = I(t)(1-(\delta t/\tau)) + g\delta V_{ox} \quad (28)$$

So, taking Eq. (28) into Eq. (26), the total conduction current $I(t)$ between nodes 'o' and 'x' can be written in a time discretized form as:

$$I_{ox,k} = g_s V_{ox,k} + (g_\alpha + g_\beta)\delta V_{ox} + (I_{\alpha,k-1} + I_{\beta,k-1}) - \left(\frac{I_{\alpha,k-1}}{\tau_\alpha} + \frac{I_{\beta,k-1}}{\tau_\beta}\right)\delta t \quad (29)$$

where k is the time discretized parameter. Following an equivalent procedure to that presented in Eqs. (3)–(9), we obtain the equation system in the matrix notation as:

$$CV = Q + F \quad (30)$$

where C is the high frequency capacitance matrix containing terms as $c_\infty = \varepsilon_o \varepsilon_\infty A/L$ (see Appendix C), V is the node potential vector, Q is the node charge vector with terms given by:

$$Q_{o,k} = Q_{o,k-1} - \sum_x I_{ox,k-1}\delta t \quad (31)$$

and F is the excitation vector given by:

$$F = \begin{bmatrix} c_{F1}V_{F1} \\ c_{F2}V_{F2} \\ \cdots \\ c_{FN}V_{FN} \end{bmatrix} \quad (32)$$

where, like Eq. (8), c_F is the capacitance connecting the source electrode to the medium. Eqs. (29)–(32) have to be solved iteratively to obtain the vectors V and Q in each time step.

6.2. Frequency domain analysis

For frequency domain analysis, Fig. 12(c) is considered the equivalent circuit of the tissue. $\sigma(\omega)$ and $\varepsilon(\omega)$ are given by Eqs. (24) and (25). The total admittance between nodes is $y = \gamma A/L$, where γ is the specific admittance defined in Eq. (18). Applying the Kirchhoff Currents Law for each one of the N nodes in the total medium equivalent circuit, we obtain N equations like this:

$$\sum_x y_{ox}(v_o - v_x) = 0 \quad (33)$$

where the summation extend over all neighbours nodes connected to the node 'o' and v is the node potential in phasor notation. Now, separating real and imaginary parts of Eq. (33) results:

$$\sum_x g_{ox}(v_{or} - v_{xr}) - \omega c_{ox}(v_{oi} - v_{xi}) = 0$$

$$\sum_x \omega c_{ox}(v_{or} - v_{xr}) + g_{ox}(v_{oi} - v_{xi}) = 0 \quad (34)$$

where the subscripts 'r' and 'i' indicate real and imaginary parts, respectively. Eq. (34) can be rewritten in the form of a matricial equation:

$$YV = F \quad (35)$$

where:

$$V = \begin{bmatrix} v_{1r} \\ v_{2r} \\ \cdots \\ v_{Nr} \\ v_{1i} \\ v_{2i} \\ \cdots \\ v_{Ni} \end{bmatrix}, \quad F = \begin{bmatrix} g_{F1}v_{F1} \\ g_{F2}v_{F2} \\ \cdots \\ g_{FN}v_{FN} \\ \omega c_{F1}v_{F1} \\ \omega c_{F2}v_{F2} \\ \cdots \\ \omega c_{FN}v_{FN} \end{bmatrix}, \quad Y = \begin{vmatrix} G & -\omega C \\ \omega C & G \end{vmatrix} \quad (36)$$

where g_F and c_F are the conductance and capacitance connecting the source electrode to the medium, respectively. G and C are the conductance and capacitance matrix of the medium. Both of them have $N \times N$ size, with the same structure of the others C matrix presented previously (and also in Appendix C). Eq. (35) has to be solved to obtain the vector V in each frequency of interest.

7. Results using the tissue scale model

Now, the example of muscle tissue excited by a electric field can be concluded. The values obtained for σ and ε inside a bundle of fibres in the β dispersion were shown in Fig. 11. The α dispersion did not appear in the numerical results because spatial resolution was very poor for modelling the electric transport in the double layer. In order to make this analysis more realistic, we are going to take some approximated values for α dispersion of dog skeletal from [2]:

$\tau_\alpha = 1.6$ ms

$\varepsilon_\alpha = 10^6$

$\sigma_\alpha = 5.5 \times 10^{-5}$ S/cm

Fig. 13 shows a piece of the tissue structure given in Fig. 4, where now the circular structures are bundles of fibres

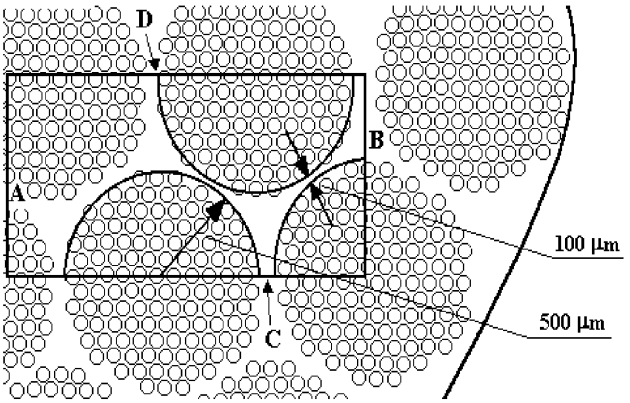

Fig. 13. View of a piece of the skeletal muscle used in the numerical simulation with the tissue scale model. Interstitial space between bundles is filled with electrolyte. Planes A and B are for source connection. Planes C and D are even symmetry surfaces where transversal field and current vanishes.

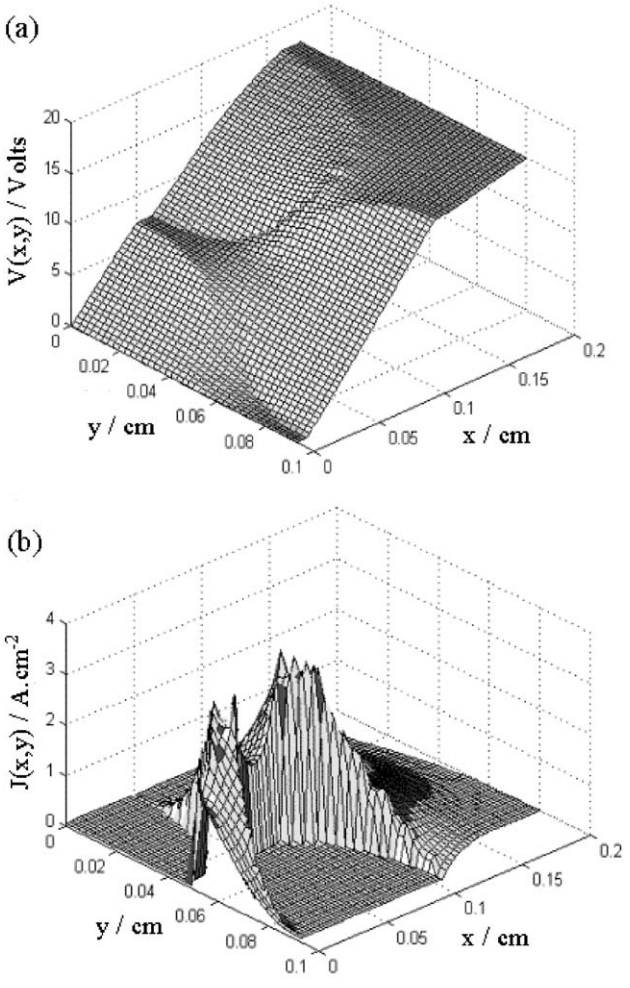

Fig. 14. Distributions of (a) electric potential and (b) total current density on the tissue for 1 Hz and 100 V/cm applied field. In low frequencies, the electric field is uniform inside the bundles and higher there than the outside, while current concentrates in the interstitial space between bundles. Inside the bundles the current does not vanish, although it does not appear in (b).

inside the muscle. The space between adjacent bundles is considered filled only with electrolyte, so that the parameters for dispersion modelling in that region are the electrolyte conductivity, $\sigma_s = 1.77 \times 10^{-2}$ S/cm and the water permittivity, $\varepsilon_\infty = 78$. No dispersion process in the electrolyte is considered.

The mesh for numerical simulation was built with $75 \times 40 = 3000$ squares with edge of 24 μm. We used frequency domain analysis in the frequency range from 1 Hz to 100 MHz.

Fig. 14 shows the potential and current distributions on the tissue for a 1 Hz and 100 V/cm electric field excitation. Note in Fig. 14(a) that the electric field is uniform inside the bundles and higher than the field outside. The current distribution in Fig. 14(b) is very concentrated in the interstitial space between the bundles. However, current inside the bundles does not vanish under 'dc' excitation.

Finally, calculating the averaged values of current and field around a bundle of fibres and using again the concept of specific admittance, we obtained the dispersion curves of the tissue. This is shown in Fig. 15. The two bands of dispersion is very well marked in the permittivity curve. This is a characteristic of the current-field relation inside the

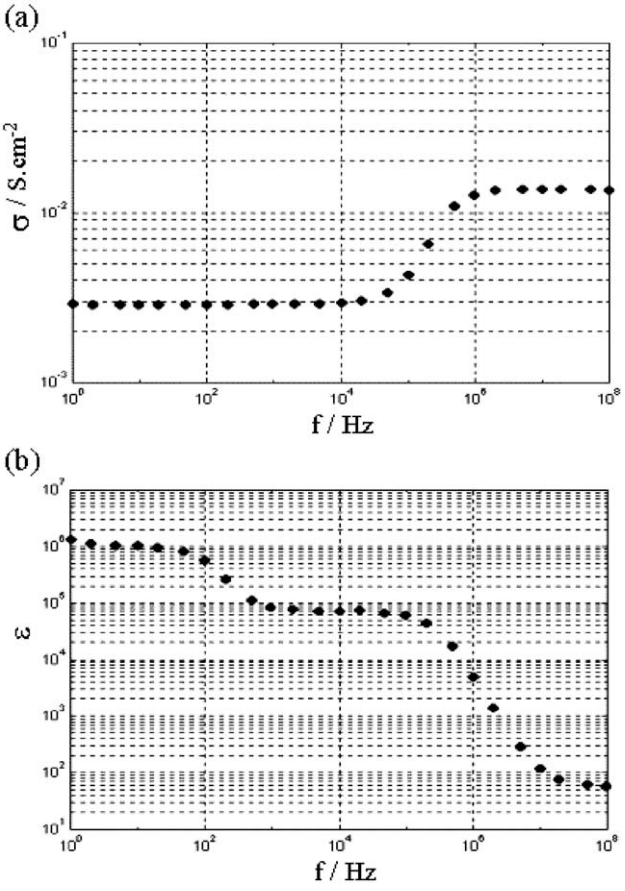

Fig. 15. Dispersion curves for the tissue. (a) Conductivity and (b) permittivity. It has well marked the two bands of dispersion in the permittivity curve.

bundles. On the other hand, the low frequency conductivity of the tissue is practically due to the interstitial conduction. Numerical results agree well qualitatively with experimental results from Ref. [2].

8. Conclusion

The equivalent circuit method was designed aiming to overcome limitations in the numerical modelling of the electrical properties of biological media linked to the local anisotropy around cell membranes and relaxation process that cause dispersion in the conductivity and permittivity of the tissues. It joins the simplicity of the finite difference approach for the electric transport differential equations, the easiness of the lumped circuit modelling and the power of the finite integration method to solve the coupled problem of charge and field in the conduction process.

The cell scale model is an approach used for local analysis around cells. In this approach, one considers only the effect of the nearest neighbours cells around the target cell. It permits to obtain spatial distributions in time steps of electrical potential, charge concentration and current density of any type of ion included in the model. That information can be very useful in experiments of electrical excitation of cells.

Although not considered in the example presented in this paper, an important feature of the cell scale model is the possibility to include non-linear effects associated with biological membranes as ionic channels and electroporated membrane conductance.

The tissue scale model utilises first order relaxation approaches to model the dispersive behaviour of tissues by means of a network of capacitance and conductance.

Since we have ignored the dielectric dispersion of the electrolyte (mainly due to the dipolar relaxation of water and proteins), the proposed method is frequency limited to the range where this effect can be neglected in relation to the dominant one associated with interfacial polarisation of the membranes. Roughly, we can state this limit at about 100 MHz.

Appendix A

In an electrolytic solution, the Nerst–Planck equation for one specific ion n can be written in the form:

$$j_n = -z_n e D_n \left(\nabla c_n + \frac{z_n e c_n}{KT}\nabla \phi_n\right) \tag{A.1}$$

where z_n is the ion valence, D_n is the diffusion coefficient of the ion, c_n is the ionic density, ϕ_n is the effective potential of that ion type in that medium, e is the proton charge, K is the Boltzmann constant and T is the absolute temperature. Defining the term $v_n = KT/ez_n$ as a constant for each ion type, we can write Eq. (A.1) according to the notation used in Eqs. (1) and (2):

$$j_n = -\mu_n(\rho_n \nabla \phi_n + v_n \nabla \rho_n) \tag{A.2}$$

where the ionic mobility μ_n is related to the diffusion coefficient by the Einstein's relation, $D_n = \mu_n v_n$ and $\rho_n = z_n e c_n$ is the ionic charge density. Eq. (A.2) can be rewritten in the form:

$$j_n = -\mu_n v_n e^{-\phi_n/v_n}\nabla(\rho_n e^{\phi_n/v_n}) \tag{A.3}$$

From now on, we are going to ignore any possible difference between the effective potentials of different ion types, so that the potential ϕ_n will be substituted by V, the potential due to the external sources and internal charge accumulation. Now, considering the discretization of the space, we can rearrange terms and calculate the line integral of both sides of Eq. (A.3) in a specific direction connecting two adjacent nodes.

$$\int_0^L j_n e^{V/v_n}\mathrm{d}l = -\mu_n v_n \int_0^L \mathrm{d}(\rho_n e^{V/v_n}) \tag{A.4}$$

j_n is now the component of the current density of the ion n in the direction of dl. Taking j_n as a constant inside the volume between the two nodes and V as varying linearly between limits 0 and L, we obtain from Eq. (A.4):

$$j_n = (\mu_n/L)\Delta V(\rho_0 e^{\Delta V/v_n} - \rho_L)/(e^{\Delta V/v_n} - 1) \tag{A.5}$$

where $\Delta V = V_0 - V_L$. In order to obtain the current of the ion n crossing the area between the nodes, we have to multiply j_n by A (the cross-sectional area between the nodes). Additionally, we can substitute ρ_0 and ρ_L by $\rho_{\mathrm{av}} + \Delta\rho/2$ and $\rho_{\mathrm{av}} - \Delta\rho/2$, respectively, where ρ_{av} is the averaged charge density and $\Delta\rho = \rho_0 - \rho_L$. So, the current is given by:

$$I_n = (\mu_n A/L)\rho_{av}\Delta V + (\mu_n A/L)\Delta\rho(\Delta V/2)(e^{\Delta V/v_n} + 1) /(e^{\Delta V/v_n} - 1) \tag{A.6}$$

Defining the factor f_n by:

$$f_n = (\Delta V/2v_n)(e^{\Delta V/v_n} + 1)/(e^{\Delta V/v_n} - 1) \tag{A.7}$$

the current of the ion n can be written in the final form:

$$I_n = g_n \Delta V + k_n \Delta\rho \tag{A.8}$$

where:

$$g_n = \mu_n \rho_{av} A/L \tag{A.9}$$

$$k_n = f_n D_n A/L \tag{A.10}$$

Note that $f_n = 1$ to $\Delta V = 0$ and $f_n \approx 0.5\Delta V/v_n$ when $\Delta V \gg v_n$.

Appendix B

The problem of a cylindrical membrane in a electrolytic solution submitted to a uniform electric field is solved here aiming to obtain a reference for numerical results evaluation. Considering that the charge density vanishes in the whole region of interest except on the membrane, one can start from Laplace's equation. In two dimensions, we have:

$$\frac{1}{r}\frac{\partial}{\partial r}\left(r\frac{\partial V}{\partial r}\right)+\frac{1}{r^2}\frac{\partial^2 V}{\partial \theta^2}=0 \tag{B.1}$$

The general solution of this equation, obtained from variables separation, is of the form:

$$V(r,\theta,t)=[s_1(t)r^m+s_2(t)r^{-m}][s_3(t)\cos(m\theta)+s_4(t)\sin(m\theta)] \tag{B.2}$$

where it is assumed that the coordinate system has its origin on the cylindrical centre. The s coefficients are functions of time only and m is a constant. All these unknown values should be determined from boundary conditions.

$$\begin{aligned} &V(r\to 0,\theta,t)\to \text{finite value}\quad V(r\to\infty,\theta,t)\\ &=rE_o\cos\theta\quad \frac{\partial q_s^+}{\partial t}=-\sigma_o\frac{\partial V}{\partial r}(r\to a^+)\\ &=C_m\frac{\partial}{\partial t}[V_{(r\to a^+)}-V_{(r\to a^-)}]\quad \frac{\partial q_s^-}{\partial t}=\sigma_i\frac{\partial V}{\partial r}(r\to a^-)\\ &=C_m\frac{\partial}{\partial t}[V_{(r\to a^-)}-V_{(r\to a^+)}] \end{aligned} \tag{B.3}$$

where E_o is the value of the uniform applied electric field. q^+ and q^- are the outside and inside surface charge density on the membrane, respectively. Naturally, $q^-=-q^+$ due to the electric flux density continuity condition. σ_o and σ_i are the outside and inside electrolyte conductivity, respectively. a is the membrane radius and C_m is the capacitance per unit area of the membrane. The notation $r\to a^+$ and $r\to a^-$ refers to the limit of $r=a+\delta$ and $r=a-\delta$ when $\delta\to 0$. Taking the time derivatives in Eq. (B.3) to the frequency domain, the application of the whole set of boundary conditions in Eq. (B.2), results in:

$$V=E''r\cos\theta \qquad \text{for } r<a \tag{B.4}$$

$$V=(E_o r+E'r^{-1})\cos\theta \qquad \text{for } r>a \tag{B.5}$$

where

$$E'=\frac{1+j\omega\ aC_m(1/\sigma_i-1/\sigma_o)}{1+j\omega\ aC_m(1/\sigma_i+1/\sigma_o)}a^2E_o \tag{B.6}$$

$$E''=\frac{j\omega 2\ aC_m/\sigma_i}{1+j\omega\ aC_m(1/\sigma_i+1/\sigma_o)}E_o \tag{B.7}$$

Taking h as the membrane thickness, the electric field on the membrane is given by:

$$E_m=\frac{V_{(r\to a^+)}-V_{(r\to a^-)}}{h}=\frac{2aE_o\cos\theta}{h}\frac{1}{(1+j\omega\tau)} \tag{B.8}$$

where

$$\tau=aC_m(1/\sigma_i+1/\sigma_o) \tag{B.9}$$

In the time domain, E_m is given by:

$$E_m=(2\ a\ E_o\cos\theta/h)(1-e^{-t/\tau}) \tag{B.10}$$

Appendix C

The admittance matrix of the equivalent circuit is obtained from the set of node equations. Applying the Kirchhoff Current Law to any node results in the following relation involving node potentials and branch admittances:

$$\sum_x y_{ox}(V_o-V_x)=\left(\sum_x y_{ox}\right)V_o-\sum_x y_{ox}V_x=0 \tag{C.1}$$

As explained previously, the number of connections of a node depends on its position in the mesh. In a three-dimensional problem with a regular mesh, this number can be 4, 5 or 6. Then, the number of terms in each node equation can be 5, 6 or 7. When the set of node equations of the circuit is put in the matrix form, the admittance matrix is formed. Assuming that every connection has the same admittance y_o, the admittance matrix of the three-dimensional regular mesh is:

$$\begin{array}{c} \begin{array}{cccccccccc} 1 & 2 & & & N_y+1 & & & N_yN_z+1 & & N_xN_yN_z \\ \downarrow & \downarrow & & & \downarrow & & & \downarrow & & \downarrow \end{array} \\ \left|\begin{array}{cccccccccc} 4y_o & -y_o & 0\ldots 0 & -y_o & 0 & & 0\ldots 0 & -y_o & 0 & 0\ldots 0 \\ -y_o & 5y_o & -y_o & 0\ldots 0 & -y_o & 0 & 0\ldots 0 & -y_o & & 0\ldots 0 \\ 0 & -y_o & 5y_o & -y_o & 0\ldots 0 & -y_o & 0 & 0\ldots 0 & & -y_o\ldots 0 \\ \ldots & & & & & & & & & \\ \ldots & -y_o & 0\ldots 0 & -y_o & & & 0\ldots 0 & -y_o & 6y_o\ -y_o & 0\ldots 0 \\ \ldots & & & & & & & & & \\ \ldots & & 0 & 0 & -y_o & & 0\ldots 0 & -y_o & 0\ldots 0 & -y_o\ 4y_o \end{array}\right| \end{array}$$

This is a square matrix with $(N_xN_yN_z)^2$ elements, where N_x, N_y and N_z are the number of nodes (or mesh division) on axes x, y and z, respectively. The only terms that do not vanish in each line of the matrix are the main diagonal term, which refers to the central node coefficient, and the terms correspondent to the nearest neighbours. Considering node numeration starting by the z axes and following by y and x axes, respectively, then in the line of the node n, the non-zero terms are located in the positions $n-1$, $n-N_y-1$, $n-N_yN_z-1$, n, $n+1$, $n+N_y+1$ and $n+N_yN_z+1$.

Because complex admittance is linearly dependent from conductance and capacitance, matrices G and C have the same structure as that of the matrix Y.

References

[1] J.C. Lin, O.P. Gandhi, Computational methods for predicting field intensity, Handbook of Biological Effects of Electromagnetic Fields, 2nd ed., CRC Press, New York, 1995, pp. 337–402.

[2] K.R. Foster, H.P. Schwan, Dielectric properties of tissues, Handbook of Biological Effects of Electromagnetic Fields, 2nd ed., CRC Press, New York, 1995, pp. 25–102.

[3] P.W. Atkins, Physical Chemistry, 5th ed., Oxford Univ. Press, Oxford, 1992, p. 837.

[4] H.P. Schwan, Electrical properties of blood and its constituents: alternating current spectroscopy, Blut 46 (1983) 185–197.

[5] K.S. Cole, R.H. Cole, Dispersion and absorption in dielectrics: I. Alternating current characteristics, J. Chem. Phys. 9 (1941) 341.